Evolution of gas and star formation in simulated dwarf galaxies

C. M. Simpson (Columbia), G. L. Bryan (Columbia), M. Mac Low (AMNH), K.V. Johnston (Columbia), B. Smith (Michigan State), S. Sharma (Sydney), J. Tumlinson (STSI)

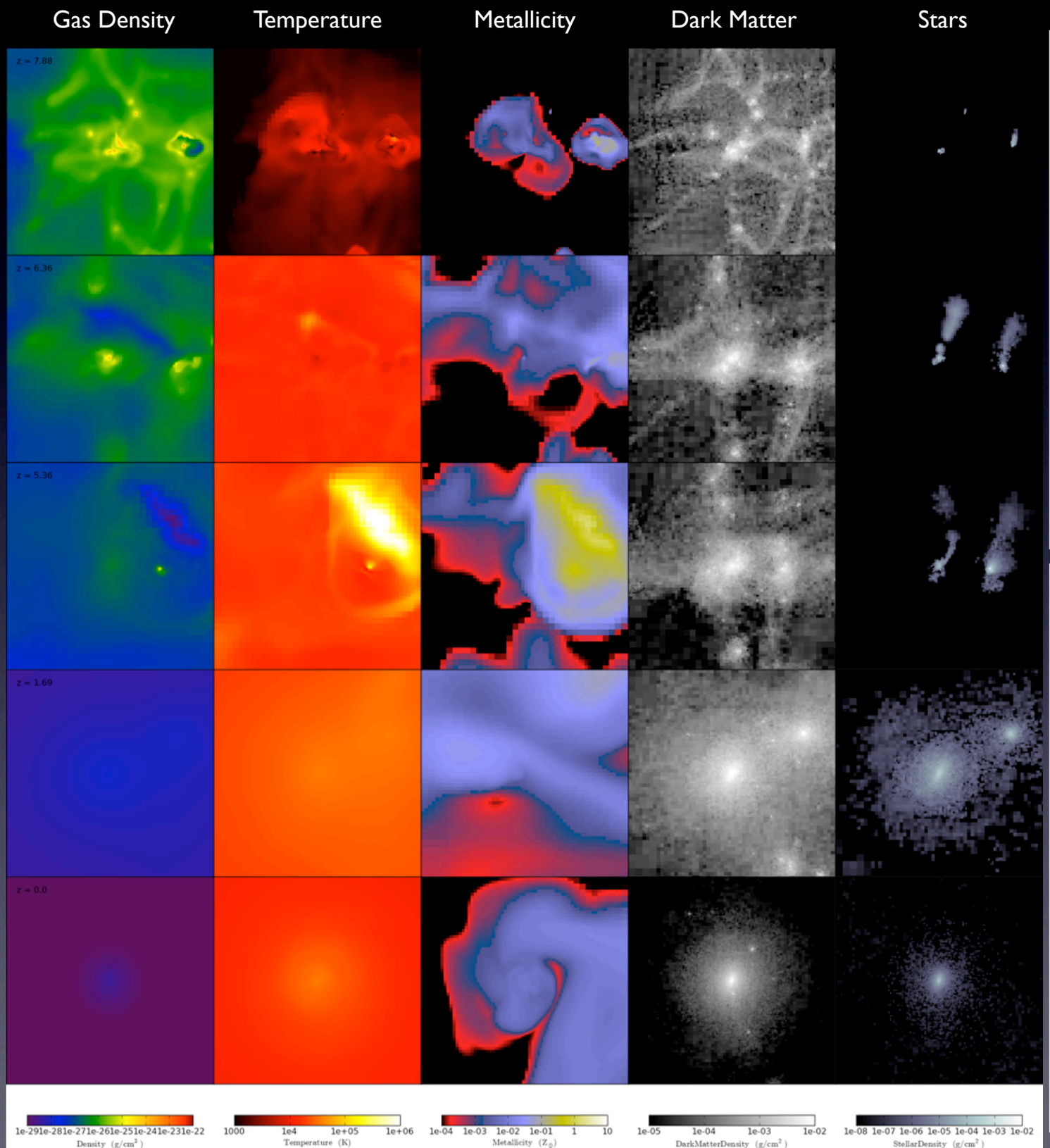

Introduction: We present a new set of cosmological, hydrodynamical simulations of dwarf galaxy formation and evolution using the AMR code Enzo. Our simulations explore the evolution of a single 10^9 $M_\odot$ halo at high resolution down to z = 0. Our maximum spatial resolution is 11 pc comoving; we refine cells that contain dark matter particles belonging to our target halo which were selected from a previously run dark matter only simulation. These cells are further refined if they meet a gas and dark matter density threshold. Our dark matter particles have a mass of 5400 $M_\odot$ and our star particles have a typical mass of 75 $M_\odot$. Our canonical simulation at this high resolution includes non-equlibrium H_2 cooling (Abel et al. 1997; Anninos et al. 1997); metal cooling (Smith et al. 2008); star formation and feedback (Cen & Ostriker 1992); photoionizing and dissociating background (Haardt & Madau 2011; Haardt & Madau 2001); and a simple self-shielding prescription. We have also run a set of simulations that varying these physical prescriptions to explore the model's sensitivity to these effects.

Figure 1: Thin projections of our canonical simulation. One progenitor of our target halo is shown at five different redshifts. The columns show (left to right) gas density, gas temperature, gas metallicity, dark matter density and stellar density. The panels in the first four rows are 15 kpc comoving wide; the panels in the last row, showing the final halo at z = 0, is $2r_{200}$ radii wide (48 kpc). All the panels have a projected depth of 5 kpc comoving. Gas density, temperature and metallically are weighted by gas density; dark matter density and stellar density are unweighted. In this simulation, a photoionizing and photodissociating background is introduced at z = 7 and gradually ramped up to full strength at z = 6. Each star particle that is created returns 10^{-6} of its rest mass energy to the gas as thermal energy as well as injecting 1 $M_\odot$ of metals (check this). We see that supernovae drive metal rich galactic winds into the IGM. This activity peaks with the star formation rate, before reionization. Once reionization occurs, gas is photoevaporated from progenitor halos and star formation gradually declines and ceases around z = 4. Gas is unable to re-cool in these halos; what remains at z = 0 is a halo that contains 10^9 $M_\odot$ of dark matter, 2×10^6 $M_\odot$ of stars and very little gas.

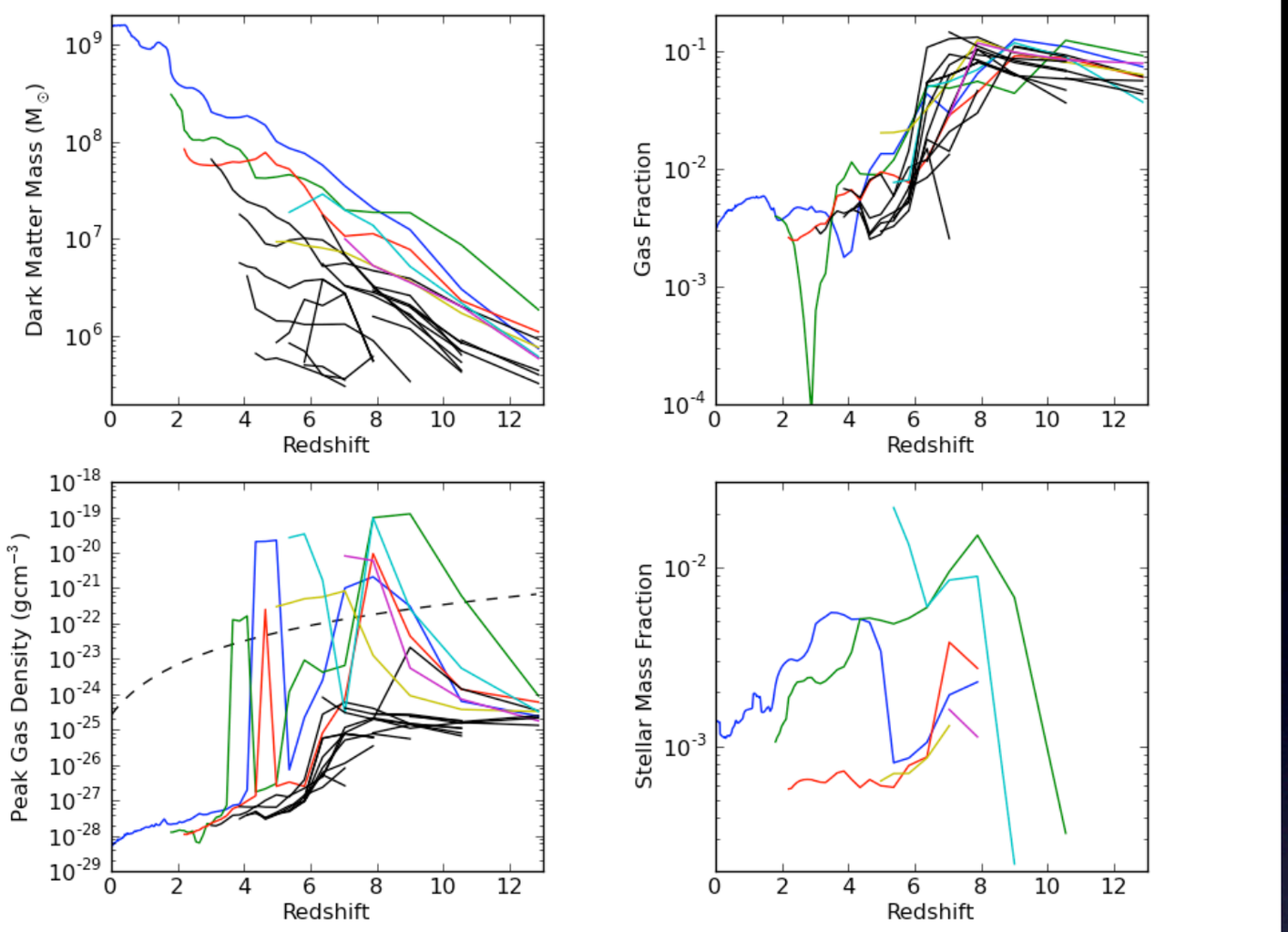

Figure 2: Like all dark matter halos in CDM simulations, our dwarf halo forms hierarchally from many lower mass progenitor halos. This figure shows the evolution of the dark matter mass, gas fraction, peak gas density and stellar mass fraction within the r200 radius at each redshift. Halos that form stars during their evolution are show with colored lines. Halos that do not form stars are shown with black lines. Lines terminate at low redshift when the halo they correspond to merge with another halo. In the plot of the peak gas density (bottom left panel), the density threshold for star formation (10^5 x mean density of the universe) is plotted with a dashed line. In addition to a density threshold, gas must also be inflowing and have a cooling time shorter than the dynamical time to form stars.

The gas fraction declines sharply between z = 6 and 7 when the photoionizing and photodissociating backgrounds are turned on. Some halos are able to maintain a component of dense gas, but by z = 4 this gas has disappeared.

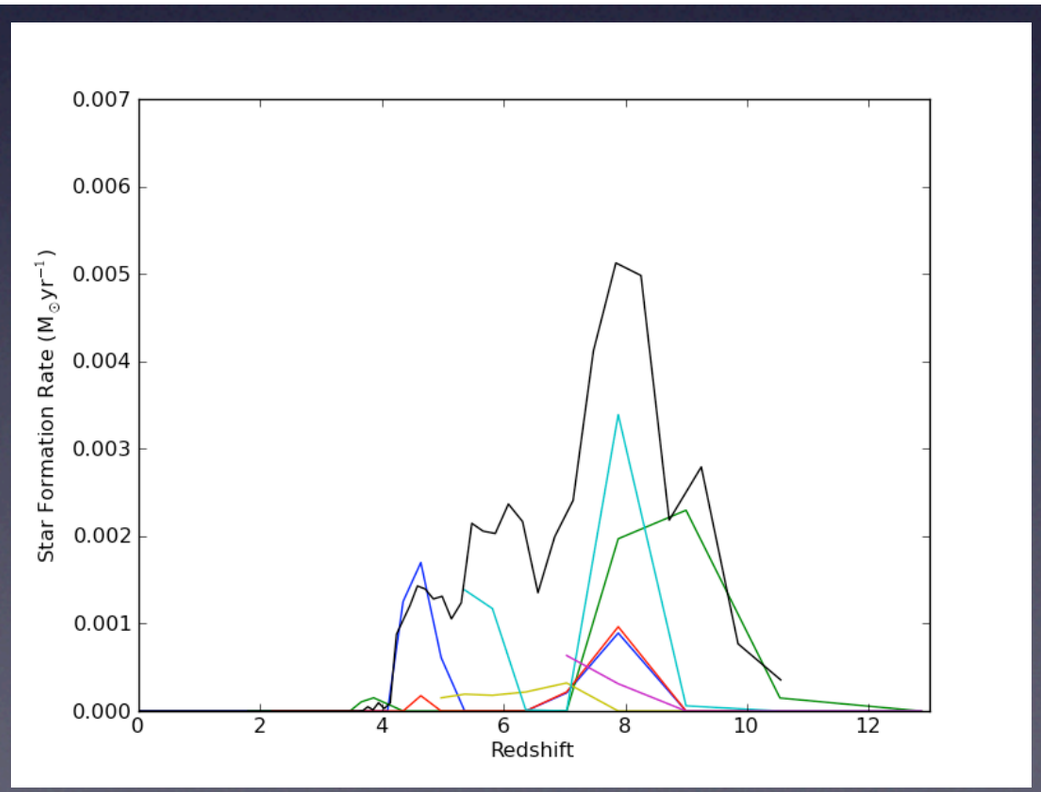

Figure 3: Star formation rate vs. redshift. There are two ways to compute the star formation rate of the target halo. One is to compute a rate from the formation time stamps on the star particles in the final halo. This rate is shown as a black line. The other way is to compute an instantaneous rate for each progenitor halo at each data output. These rates are shown as colored lines. The colors correspond to the same halos as in Figure 2. The star formation history is quite bursty, with multiple halos undergoing bursts that contribute to the final stellar population.

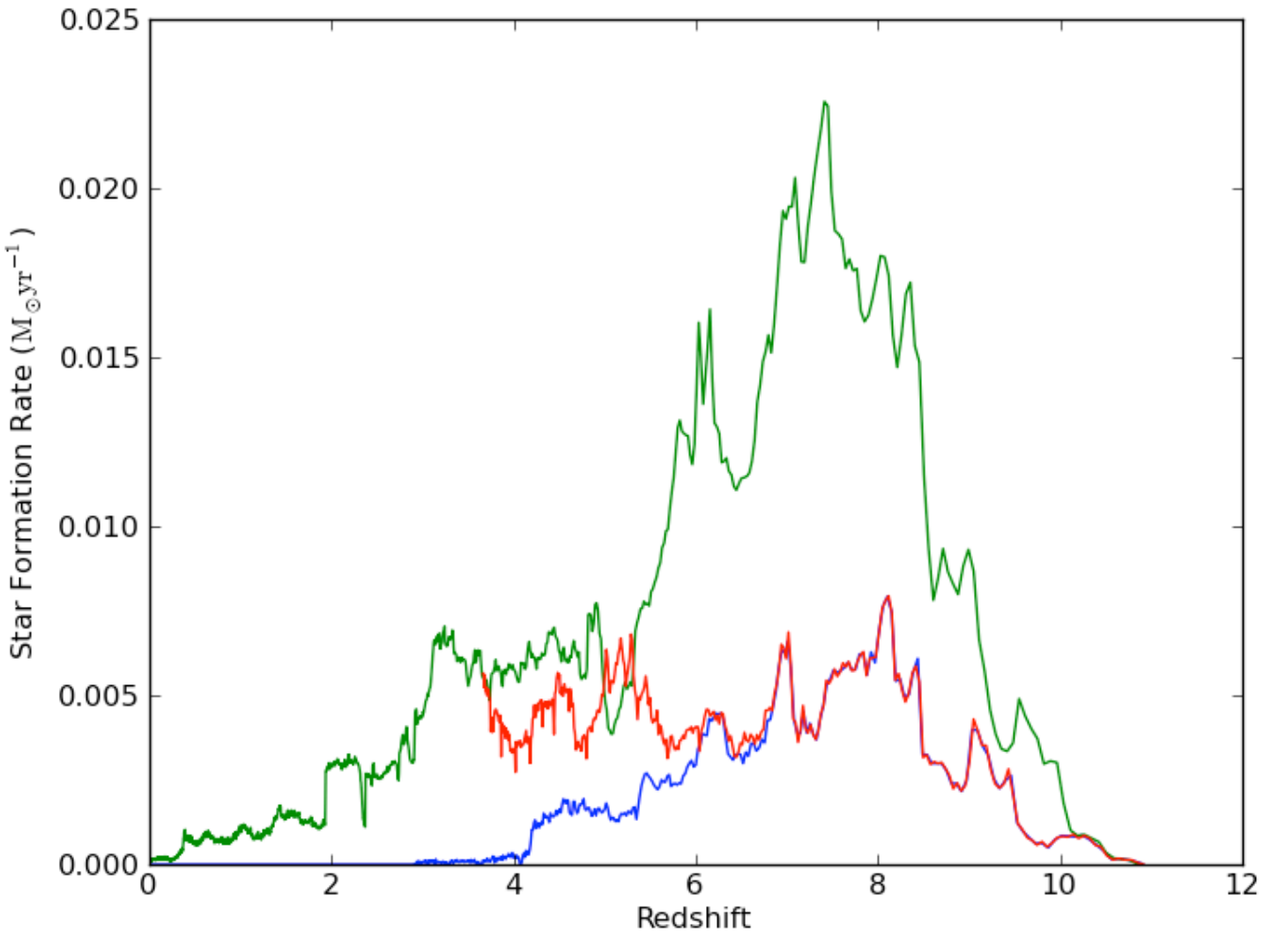

Figure 4: Star formation rate vs. redshift for the entire simulation box for three simulations with different feedback and UV background prescriptions. The blue line is for the simulation presented in Figures 1, 2 and 3. It includes photoionizing and photodissociating backgrounds that turn on between z = 6 and 7 and supernovae feedback. The green line is a simulation that includes both UV backgrounds but does not have any thermal feedback from supernovae. Metals are still injected by star particles as they would with supernovae, however, the metal cooling rates are limited in cells where the metallicity exceeds 0.01 Zsun. The red line is a simulation that includes thermal feedback from supernovae, but does not include either UV background. This run has only been run up to z = 3.6.

These runs demonstrate that it is neither supernovae feedback nor reionization that is responsible for quenching star formation in our canonical model. Thermal energy injection from supernovae seems to set the level of star formation within the progenitor halos, but it is reionization that produces initiates the overall decline in the star formation rate.

Conclusions and Future Work: We have conducted the first cosmological simulations of dwarf galaxy formation and evolution run to z = 0 with an AMR code. Like similar studies conducted with SPH codes (Sawala et al. 2010) and high redshift studies with AMR codes (Gnedin & Kravtsov 2006), we have found that supernova feedback and reionization play important roles in the evolution of halos of this mass. We find that supernovae feedback regulates the efficiency of star formation, but reionization is the effect that produces an overall decline in the star formation rate and is the effect that quenches star formation. We also find that like halos of larger mass, dwarf halo formation is a messy, hierarchal process. We find that all the halo progenitors stop forming stars around z = 4. Resolved stellar populations of local group and milky way dwarf galaxies show many are dominated by older populations, but many have younger populations as well (Weisz et al. 2011). What produces these late forming populations may be indicative of higher viral masses for these galaxies, different assembly histories, different environments or some piece of physics we have not considered in our model. We plan to make our model more complex in the future by including a prescription for local UV heating and further increasing resolution. We also plan to conduct multiple realizations of halos at several different masses. We ultimately plan to implement an algorithm for the formation of individual stars and track multiple chemical species.

Abel, T., Anninos, P., Zhang, Y., & Norman, M. L. (1997). Modeling primordial gas in numerical cosmology. New A, 2, 181–207.

Anninos, P., Zhang, Y., Abel, T., & Norman, M. L. (1997). Cosmological hydrodynamics with multi-species chemistry and nonequilibrium ionization and cooling. New A, 2, 209–224.

Cen, R. & Ostriker, J. P. (1992). Galaxy formation and physical bias. ApJ, 399, L113–L116.

Gnedin, N. Y. & Kravtsov, A. V. (2006). Fossils of Reionization in the Local Group. ApJ, 645, 1054–1061.

Haardt, F. & Madau, P. (2001). Modelling the UV/X-ray cosmic background with CUBA. In D. M. Neumann & J. T. V. Tran (Ed.), Clusters of Galaxies and the High Redshift Universe Observed in X-rays.

Haardt, F. & Madau, P. (2011). Radiative transfer in a clumpy universe: IV. New synthesis models of the cosmic UV/X-ray background. ArXiv e-prints.

Sawala, T., Scannapieco, C., Maio, U., & White, S. (2010). Formation of isolated dwarf galaxies with feedback. MNRAS, 3–+.

Smith, B., Sigurdsson, S., & Abel, T. (2008). Metal cooling in simulations of cosmic structure formation. MNRAS, 385, 1443–1454.

Weisz, D. R., Dalcanton, J. J., Williams, B. F., Gilbert, K. M., Skillman, E. D., Seth, A. C., Dolphin, A. E., McQuinn, K. B. W., Gogarten, S. M., Holtzman, J., Rosema, K., Cole, A., Karachentsev, I. D., & Zaritsky, D. (2011). The ACS Nearby Galaxy Survey Treasury VIII. The Global Star Formation Histories of 60 Dwarf Galaxies in the Local Volume. ArXiv e-prints.